FIELD TESTS FOR ICEBERG IMPACT LOADING

by

S.E. BRUNEAU[1], A.B. CAMMAERT[1], AND K.R. CROASDALE[2]

[1] C-CORE - Centre for Cold Ocean Resources Engineering
Memorial University of Newfoundland
St. John's, NF, Canada
A1B 3X5
Tel: (709) 737-7900 Fax: (709) 737-4706

[2] K.R. Croasdale and Associates Ltd.
334, 40th Avenue S.W.
Calgary, AB, Canada
T2S 0X4
Tel: (403) 243-7787 Fax: (403) 287-7889

ABSTRACT

Some level of ice tolerance will determine operating efficiency and safety of both fixed and floating production systems off Canada's East Coast. For floating production systems large icebergs will be avoided, but impacts from bergy bits and growlers which may escape detection and management systems will govern local design.

This paper describes the results of a pilot experimental program aimed at advancing the understanding of ice/structure interaction processes, and the loads and pressures produced by small iceberg impacts on offshore structures. The field program was conducted in Newmans Cove, Bonavista Bay, Newfoundland, during the spring of 1992. The experimental program was the first in which natural iceberg pieces were drawn into a shore based, instrumented, load measurement system for the purposes of recording impact loads, kinematics, and ice crushing characteristics. Detailed data analyses of iceberg characteristics, drag coefficients, kinematics, force traces, contact areas, and pressure/area relationships have been performed. This paper reviews the analysis of measured force time histories contact areas and resultant pressure calculations. Significantly, these results indicate lower ice loads than those which would have been determined using the existing knowledge base.

INTRODUCTION

Calculation of design ice loads for fixed and floating offshore structures is a complex procedure, requiring accurate information on the probability of ice impacts, the dynamics and hydrodynamics of the structure and ice feature, and the mechanical behaviour of the ice. It has been well established that the average ice pressure on a structure decreases as the nominal contact area increases, but the exact nature of the relationship has never been determined. This "scale effect" makes it extremely difficult to calculate full-scale impact loads from small and medium scale laboratory and field tests. The scale effect introduces the greatest uncertainty in the calculation of design ice loads for offshore structures. This uncertainty necessitates conservative design practices, and reduced cost-efficiency.

There is a practical limit to the size of ice sample that can be tested using conventional test frames. In order to extend the pressure/area curve to larger contact areas, indentation tests have been conducted. While these tests have yielded data on average and peak pressures associated with contact areas of up to approximately 3 m^2, information on pressures resulting from much larger contact areas is still required. Also, the indentation tests do not closely approximate the physical conditions of actual ice impacts. The indentor speeds are too low, and the ice crushing is more tightly confined than in most real impacts. Both of these factors will have a significant effect on the resulting load. In order to better understand the scale effect, and to quantify the pressure/area relationship at large contact areas, it is necessary to conduct an experiment with realistic impact dynamics, and large contact areas.

The best method of achieving realistic impact dynamics and large contact areas is direct impact testing. In these tests a floating ice feature is towed directly into a fixed, instrumented impact face. Global loads and local pressures are measured at the impact face. Since the ice features are unaltered, the ice shape (and confinement at the impact location), and temperature profiles closely resemble ice characteristics during natural iceberg/structure interactions. Also, ice motions, and ice velocities are much closer to those of a natural impact, than can be achieved with indentor tests.

Summary of Newmans Cove Experiments

In the Spring of 1992 C-CORE (The Centre for Cold Ocean Resources Engineering) conducted a pilot series of iceberg impact experiments at Newmans Cove, Newfoundland (48° 34' N, 53° 10' W Figure 1). A detailed description of the experiment site, the load panel used to measure impact loads, the data acquisition system, and other general aspects of the experiment is given in Cammaert et al. (1993a). This program involved towing small glacial ice pieces into a purpose-built steel load panel attached to the end of the local wharf. The panel was rectangular in shape, approximately 6.7 m by 2.2 m and hinged at the bottom (Figure 2). The global loads from an impact where measured via two load cells near the top of the panel. Contact areas were measured using sheets of bubble wrap packaging material stapled to plywood sheets and fixed to the front face of the panel. In total 8 impacts were obtained. These are labelled A1, B1, C1, D1, D2, E1, E2, and E3, the letter specifying the specific iceberg specimen used. Table 1 lists several of the important results from the analysis of each interaction event. This table will be referred to on several occasions and the specific row identified for each of the relevant topics being discussed. The table summarises the steps for determining the impact pressures as a function of contact area - a topic to be discussed later. The first step in the analysis is the identification of the various components of the load trace which leads to better understanding of the hydrodynamics, kinematics and ice mechanics in general. Eventually the peak ice impact force and corresponding contact area will be isolated and plotted on the pressure/area curve.

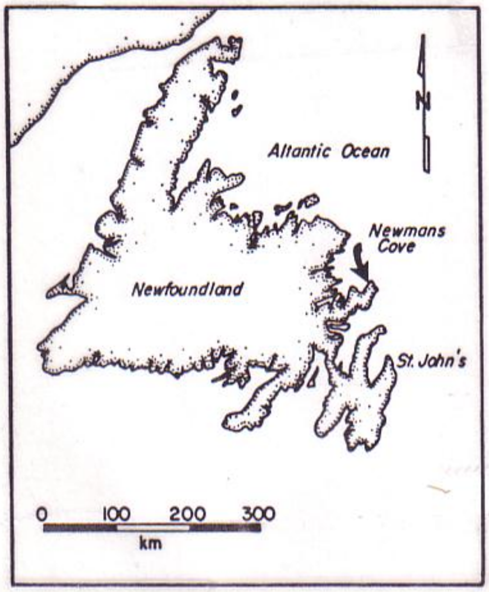

Figure 1 Location map showing experiment site.

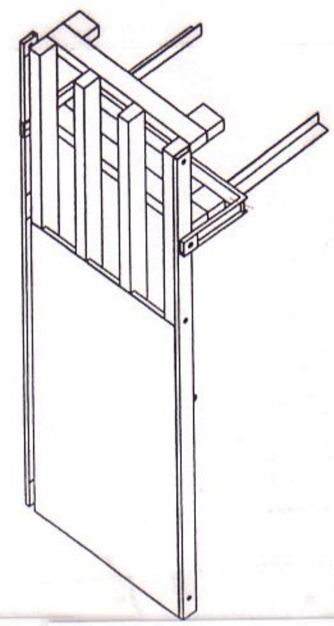

Figure 2 Sketch of the load panel

Test		A1	B1	C1	D1	D2	E1	E2	E3
Mass	kg	9650	8430	7420	9720	9720	22342	22342	22342
Speed	m/s	0.55	0.82	0.73	1	0.97	0.92	1.1	1.19
Attack angle	deg.	15	15	25	40	0	35		35
Rotation Before Impact		0	0	high	none	0	0	unk	0
Approx. Local Ice Shape		elliptic	elliptic	blocky	pyramidal	blocky, rect	wedge, rect	elliptic	irregular
Load Cell 1	kN	44.322	14.675	3.719	2.08	10.409	12.277	6.375	43.163
Load Cell 2	kN	9.323	10.146	13.993	5.666	9.64	52.235	9.988	26.341
Beam Factor		1.579	2.211	1.932	1.552	1.791	1.649	2.771	1.816
Measured Force	kN	84.70546	54.87923	34.21958	12.02179	35.90776	106.3803	45.34187	126.2193
Approximate Duraton	s	0.143	0.157	0.164	1.21	0.094	0.203	0.5	0.5
Impulse Ratio (T = .111)		1.288288	1.414414	1.477477	10.9009	0.846847	1.828829	4.504505	4.504505
Dynamic Magnif. Factor		1.6	1.5	1.5	1	1.7	1.3	1	1
Final Force	kN	52.94091	36.58615	22.81306	12.02179	21.12221	81.83099	45.34187	126.2193
Nominal Area	m^2	0.01406	0.05636	0.03161	0.035	0.03645	0.0837	0.01901	0.09641
Resultant Pressure	kPa	3.765356	0.649151	0.721704	0.34348	0.579485	0.97767	2.385159	1.309193
Aspect Ratio		0.39	0.44	0.72	0.27	0.22	0.47	0.18	0.7
Orientation of Long Axis	deg	13	43	28.5	0	5.5	53	73	90

Table 1 Summary table for Newmans Cove data analyses.

INTERACTION FORCES AND CONTACT AREAS

The load time history of each ice/structure interaction has been analyzed. The findings suggest that the load histories are comprised of several basic elements. These include the impact event (panel-ice interaction), the dynamic response of the panel to the impact event, and a significant phase-shifted hydrodynamic loading event (See Figure 3 for impact test A1). These are superimposed over a small experimental pre-tension load on the panel and gain offset on the data acquisition system. Modest background loads from wave action and mechanical and environmental noise are present in some records. Despite the consistent appearance of these basic elements in all of the load traces it appears that there are widely varying interaction conditions leading to fundamentally different ice failure mechanisms and hydrodynamic disturbances during the "impact phase" of the interaction.

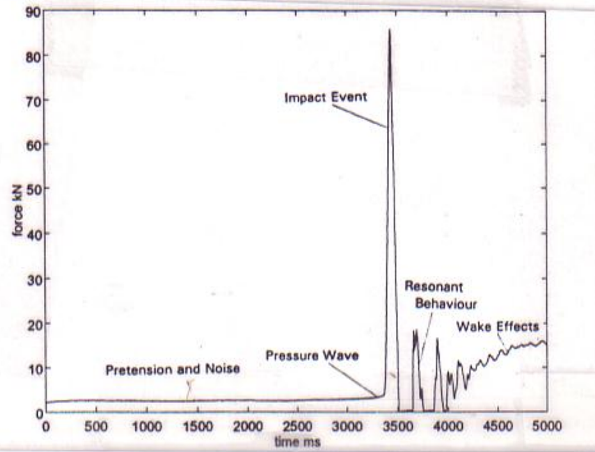

Figure 3 Recorded load trace for impact test A1.

A close look at the recorded impact for test A1 will be used to illustrate the basic elements of the load traces which are common to all tests. The variation observed in the impact phases necessitates the use of several tests for illustration in that discussion.

Force Trace Analysis

i) Pretension and Background Interference

The pretension load was applied to the compression load cells to ensure that the load panel maintained contact with the load cells throughout an interaction. This was achieved by means of tightening turnbuckles placed on cables which spanned between the top of the panel to the wharf-mounted support structure. It has been shown that the panel did loose contact with the load cells during several of the experimental impacts during periods of panel reflection after the impact event. Low level background noise can be detected in the load trace for experiment A1. The form tends to be periodic which suggests that the source of these pressures was the modest wave action at the wharf.

ii) Pressure Wave.

It is not difficult to identify the effects of the impact on the time series records. In the case of A1 it can be shown that a sharp sudden increase in the load took place at the 3.4 second mark. However, on very close inspection it is difficult to detect the exact instant at which the ice made contact. This is likely due to the minute area over which ice crushing initiates and the presence of a "bow wave" which leads the towed ice feature. The region of high pressure and resulting surface interference reach the panel before the ice piece itself. The load resulting from this fluid pressure and flow can be expected to vary in accordance with ice feature shape, Reynold's Number, and Froude Number.

iii) Impact Event

In order to study the mechanics of the ice crushing phase of each interaction, they have been extracted from the respective time histories and studied in detail. Furthermore, each impact event has been observed repeatedly via an overhead video record of the tests. Conditions range from somewhat confined direct central impacts which result in very little flaking, a short duration, and a high peak load (for example A1 and D2), to eccentric, oblique impacts in which much flaking occurs during the relatively long duration, low magnitude, fluctuating load event (D1).

For test A1 Figure 4 represents the "load impulse" portion of the interaction for which the power spectrum is also provided. Note the presence of high energy levels at a frequency of approximately 10 Hz; close to the natural frequency of the structure. Very little energy is present at high frequencies. This may be due to the inability of the structure to respond at these frequency levels. Although the load trace for test A1 is smoother and more symmetric than most others these spectral trends persist for all of the eight traces similarly analyzed.

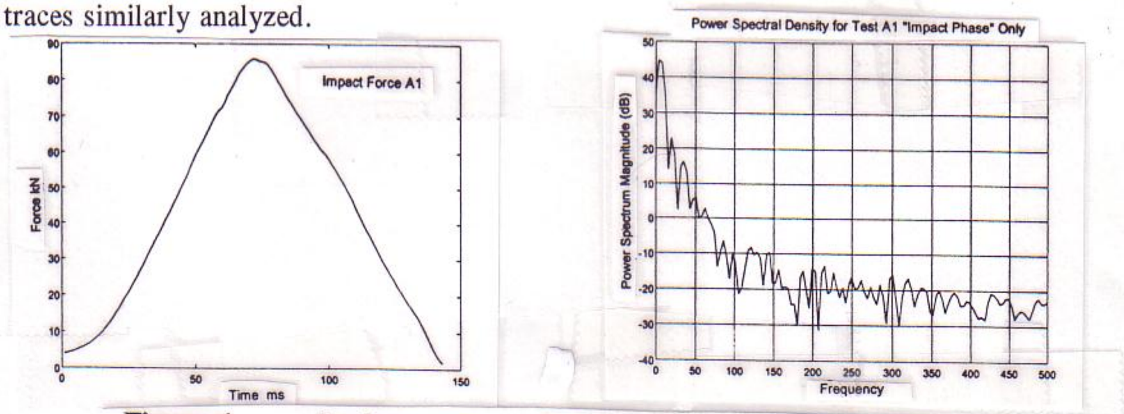

Figure 4 Ice Impact traces for A1 with power spectral density.

Figure 5 illustrates the similarities and differences between the load traces from impact D1 and impact D2. Significantly, both traces (from the same ice feature with similar momentum) exhibited the same basic trends in the load trace outside of the impact phase.

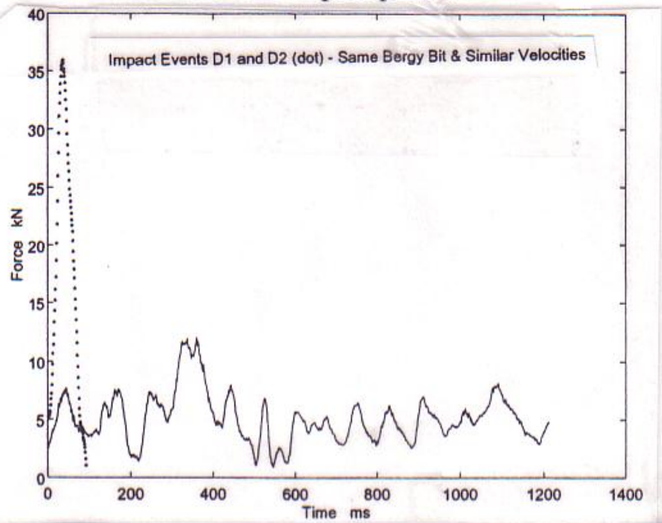

Figure 5 Superimposition of impulse phases for tests D1 and D2.

The peak measured loads for each of the impact time series records are listed in Table 1. These values are the result of adding the calibrated response of each load cell and using basic beam theory to work out the load at the point of impact on the panel. It is important to note here that the load traces analyzed represent the elastic response of the panel to an impact, not the actual applied ice loads and that the magnitudes of the loads are modified (amplified) somewhat by the structure as follows:

The result of short impulsive loads on a structure is that damping has little time to act to control the maximum displacement or acceleration response of the structure. Thus, the product of the mass and acceleration must be equal in magnitude to the elastic spring force (the stiffness constant (k) times velocity). Since impulsive loads are characterized by sudden steep increases in load (acceleration), it often results in an amplification of loads in the structure by an amount known as a dynamic magnification factor. For engineering purposes the maximum effect to be expected from impulsive loading on single degree of freedom structures can be found from plots of response spectra. These represent the dynamic magnification factor versus the ratio of impulse duration to the structures natural period of vibration. These exist for various forms of impulsive loads (Clough and Penzien, 1975). The values of dynamic magnification factor based on the observed fundamental frequency of the structure (9 Hz in bending), and the basic half sine shape of the impulse as plotted earlier, are also listed in Table 1 as are the corrected peak loads.

Note that for an impulse of very short duration a large part of the applied load is resisted by the inertia of the structure, and the stresses which are produced in the structure are much smaller than those due to longer duration impulses. In the case of the Newmans Cove impacts this meant that any applied impulse with frequency 60 Hz or greater would reduce structural response magnitude by a factor of two or more.

In summary the frequency of the load peaks is consistently near to the fundamental vibration frequency of the panel (about 9 Hz). This makes it difficult to extract any information on the periodicity of the ice crushing process as it appears that the observed dominant frequency is partially an artifact of the structure.

iv) Dynamic Response

The free vibrations of the load panel which follow the impact event are significantly damped. This is largely due to viscous effects on the submerged portion of the panel, but also results from the compliance of the load panel support structure. The dynamic response characteristics of the load panel in its deployed position has been determined analytically. The first (fundamental) and third modes of vibration in bending have been approximated by the closed form solution for a simply supported beam. Note that the stiffness of the load panel was computed via the parallel axis theorem, and was based on the material properties of the structure. However, the effective mass of the structure was determined by adding the distributed mass of the panel structure to the hydrodynamic added mass as determined for the panel shape and size. The added mass term was determined neglecting considerations for motion frequency and amplitude.

The natural frequency for the fundamental mode of vibration as determined above was approximately 9.2 Hz. This matched with the 8.9 Hz determined by video records and dominant in the resultant force time series records. However, a closer inspection revealed that the frequency recorded by the individual compression load cells was half of this (4.5 Hz). The vibrations were 180° out of phase, producing an apparent resonant frequency of 9 Hz for the combined case. It is believed that the fundamental mode of vibration in bending may only be partially responsible for the individual load cell readings, and that dissimilar restraining tensions in the cables, uneven underwater footings, or eccentric hits are causing a combined torsion/bending deflection of the panel. The detailed analysis of this system required for determining exact loading mechanics is undermined by the absence of cable tension information, foundation stiffness and structural placement and fabrication tolerances. Therefore, panel dynamics have been appraised with the best available information and judgement based on all circumstances for each test.

v) Bubble Effect.

In the case of impact A1, in which no secondary strikes were recorded and the ice feature did not slide on the panel or rotate afterwards, the recorded result showed a large increase in load well after the ice interaction. Its form, though not completely evident in A1, is roughly characterized as that of a single half-sine wave rising from zero value shortly after the impact event. It has been hypothesized that this high energy event (load reaching 10-20% of the maximum impact load but 10 times longer duration) is due to the wake structure of the ice feature. The near steady-state high Reynold's Number (Re) conditions which exist up to the point of impact between the ice and panel give rise to a flow and wake structure of considerable length and sectional area. More specifically, the presence of a recirculating "flow bubble" immediately behind bluff obstacles at similar Re is well documented (Fail et al., 1959). For a bluff body similar to the A1 ice feature, it has been calculated that the volume of water captured within this recirculating ellipsoidal bubble may be of the order of 5 times the body volume. Rough calculations indicate that the flow bubble behind a bluff obstacle of the size of the A1 ice feature would be in the range of 58 m^3. It has been shown that an ellipsoidal body of water of the order of 30 m^3 travelling at 0.55 m/s (ice velocity relative to panel) will impart over a duration of 1 second a maximum load of 13 kN (using impulse momentum considerations). This is the maximum load of the "bubble effect" in the time series records. The reason for the apparent loss of water volume is likely the result of a few experimental realities, namely that ice features with volumes of 10 m^3 would have had a significant portion (20-40%) of the volume of the recirculating bubble missing as a result of the penetration of the surface. The shape of the ice feature and its non-uniform approach velocity while under tow are also considerations. Further reductions in the expected impulse of the translating fluid may also occur because the projected area of the load panel is less than that of the flow bubble.

Contact Areas

As a means of establishing the contact areas for each bergy bit impact, bubble wrap was strategically placed over the face of the load panel. It was supported by a plywood sheet and replaced after each impact event. Thus the impression left on the bubble-wrap sheet was the integration of all contacts made during a single interaction. Although the peak force corresponded to the greatest contact area, there were cases in which rolling and sliding took place. For these cases, areas associated with peak loads were obtained through correlating the bubble wrap impressions to load traces and the overhead video record.

It was determined experimentally that individual bubbles break or tear readily when an uneven shear force is applied. Remarkably, however, in controlled laboratory testing under uniaxial compressive stress the mean bubble resistance was near 10 MPa. For groups of bubbles that number increased to 13 MPa. Though highly variable (standard deviation of 5 MPa) this attribute confirmed that in the cases of direct central impacts, bubbles within the nominal contact area which were unbroken may have been heavily loaded and therefore should be included in the contact area calculation. Table 1 lists these resultant "nominal" contact areas.

The relationship between the apparent degree of confinement and the pressures developed for each interaction has been examined. From the seemingly random shaped impressions of nominal contact area aspect ratios and long axis orientations have been determined. The aspect ratio has been defined as "width divided by length" where the length is the dimension of the longest strait line inscribed within the contact zone, and the width is the longest line fully inscribed and perpendicular to the length. The long axis orientation is the inclination of the "length" to the horizontal plane. Table 1 lists the aspect ratios orientations for each impact. The upper and lower bounds of the aspect ratio were found to be 0.72 and 0.18 respectively. These numbers may be useful in analytical procedures since for the purposes of modelling contact area growth either a wedge-shaped or an ellipsoid indentor (of eccentricity defined by the aspect ratio outlined above) may be appropriate. It appears that a strong relationship exists between the orientation of contact areas for impacts with the same ice feature, however, when all impacts are viewed a near uniform distribution of long axis orientation to the horizontal exists. In fact, what is most remarkable about this result is the uniformity. The orientations ranged from 0° to 90° and there were no intervals greater than 20°. Furthermore, the apparent trend of orientation for contact shapes from the same ice feature may not be a natural tendency. Since towing and handling procedures for a given ice piece were repeated, it is possible that the same region (though not the same point) of the bergy bit was struck repeatedly. This could not be fully established from the data set.

CONCLUSIONS

This paper reviews a detailed analysis of the iceberg impact data collected at Newmans Cove, Newfoundland, during the spring of 1992 (Cammaert et al., 1993a). The analysis has revealed considerable new information on the pressure/area relationship for ice crushing, the dynamics of the interaction between floating ice pieces and structures, and the use of instrumented load panels for ice impact experimentation. The most significant conclusions which can drawn the Newmans Cove data set can be summarized as follows:

- Towed impacts provide accurate representation of ice crushing elements of ice/structure interaction.
- The complete load traces are made up of distinct components; pretension, ice impact, structure response, and a hydrodynamic wake effect.
- Peak loads are influenced to a large extent by local ice indentation shape, degree of rotation, and hydrodynamics.
- Careful analysis of the dynamic response of the load measurement panel should be part of the experimental design process.
- The value of ice crushing strength C required to match the $P=C \times A^{-d}$ relationship with the Newmans Cove data is lower than values commonly proposed for crushing strength.

ACKNOWLEDGEMENTS

The authors gratefully acknowledge the financial support provided for this study by The National Energy Board, National Sciences and Engineering Research Council, Gulf Canada Resources Ltd, Esso Resources Canada Ltd, Chevron Canada Resources and Petro Canada Resources Limited. The authors would also like to thank Dr. Greg Crocker for his valuable contributions to this work.

REFERENCES

Cammaert, A., Bruneau, S., Crocker, G., Guzzwell, J., and Morey, B. (1993) Field Tests for Iceberg Impact Loading: Final Report Phases 2 and 3. Contract Report for National Energy Board, C-CORE Contract Number 93-C3.

Clough, R. and Penzien, J. (1975) Dynamics of Structures. McGrath/Hill, USA, Ch. 6.

Fail, R., Lawford, J., and Eyre, L., (1959) Low speed experiments on the wake characteristics of flat plates normal to an air stream. Aeronautical Research Council, Ministry of Supply, U.K.

Sanderson, T. (1988) Ice Mechanics: Risks to Offshore Structures. Norwell, MA, Graham and Trotman Inc.